FABRY-PÉROT RESONANCE OF COASTAL WATER WAVES: COMPARISON OF LINEAR MODELING APPROACHES

Jie Zhang, Michel Benoit

16èmes Journées de l'Hydrodynamique
27-29 novembre 2018 - Marseille

RÉSONANCE DE FABRY-PÉROT APPLIQUÉE AUX VAGUES CÔTIÈRES : COMPARAISON D'APPROCHES DE MODÉLISATION LINÉAIRES

FABRY-PÉROT RESONANCE OF COASTAL WATER WAVES: COMPARISON OF LINEAR MODELING APPROACHES

J. ZHANG[(1)], M. BENOIT[(1)]
zhang@irphe.univ-mrs.fr ; benoit@irphe.univ-mrs.fr

[(1)] Institut de Recherche sur les Phénomènes Hors Équilibre (Irphé),
UMR 7342, Aix-Marseille Univ, CNRS, Centrale Marseille, Marseille, France

Résumé

Lorsque des vagues périodiques se propagent dans un milieu de profondeur d'eau uniforme hormis sur une zone présentant une série d'ondulations régulières, de type rides, une réflexion importante des vagues incidentes peut se produire dans certains cas. Ce phénomène, appelé résonance de Bragg, se produit d'après la théorie linéaire asymptotique établie par Mei (1985) [6], lorsque la longueur d'onde des vagues est exactement le double de la longueur d'onde des ondulations du fond. Récemment, Couston *et al.* (2015) [1] ont étendu cette théorie au cas de deux zones de rides séparées par une zone de profondeur uniforme et montré que sous certaines conditions une amplification importante des vagues peut se produire dans la zone entre les rides (résonateur) : ce phénomène correspond à la résonance de Fabry-Pérot initialement étudiée en optique. Dans ce travail, nous étudions par le biais de simulations numériques (réalisées avec la version linéaire du code potentiel de vagues whispers3D), les effets de certaines des hypothèses de la théorie ALAT, notamment pour ce qui est de la formulation de la condition à la limite sur le fond ondulé. Nous montrons en particulier que lorsque l'amplitude relative des rides augmente, la résonance de Fabry-Pérot se produit pour un nombre d'onde des vagues incidentes légèrement plus faible que celui prédit par ALAT ('wave number downshift'). La forme de la courbe de résonance est également étudiée, et il apparaît que la gamme de nombres d'onde susceptibles d'entrer en résonance est réduite, et ce d'autant plus que l'amplitude relative des rides augmente.

Summary

When periodic waves propagate in a medium of uniform water depth except on an area having a series of regular ripples, significant reflection of the incident waves can occur in some cases. This phenomenon, called Bragg resonance, occurs from the asymptotic linear

theory established by Mei (1985) [6] when the wavelength of the surface waves is exactly twice the wavelength of the bottom ripples. Recently, Couston *et al.* (2015) [1] extended this theory to the case of two patches of ripples separated by a zone of uniform depth and showed that under certain conditions a significant amplification of the waves can occur in the zone between the patches (resonator): this phenomenon corresponds to the Fabry-Pérot resonance initially studied in optics. In this work, we study, through numerical simulations (carried out with the linear version of the potential wave code whispers3D), the effects of some of the assumptions of the ALAT, in particular with regard to the formulation of the bottom boundary condition. We show in particular that when the relative amplitude of the ripples increases, the Fabry-Pérot resonance occurs for a slightly lower incident wave number than that predicted by ALAT ('wave number downshift'). The shape of the resonance curve is also studied, and it appears that the range of wave numbers likely to come into resonance is reduced, especially as the relative amplitude of the ripples is increased.

I – Introduction

Since the 1970s, it has been observed that when water waves propagate over the a patch of sinusoidal corrugations on an otherwise flat bottom, significant reflection of the incident waves can be observed under certain conditions. When the incident wavelength is twice than that of the bottom ripples, the so-called 'Bragg resonance' may take place. This phenomenon has been confirmed experimentally in wave flume experiments by Heathershaw (1982) [4] and Davies & Heathershaw (1984) [3].

In the linear framework, Davies (1982) [2] and Mei (1985) [6] have developed mathematical models to describe linear incident wave propagating over a series of ripples on an otherwise flat bottom. In both models, the amplitude of the free surface elevation as well as the amplitude of the bottom ripples are assumed to be small. It is known that Davies model can only predict non-resonance cases with a small number of bottom corrugations, whereas Mei's asymptotic linear analytical theory (ALAT) [6] is capable to describe the resonance.

Recently, Couston *et al.* (2015) [1] considered water wave trapping by using the analogous mechanism to the Fabry-Pérot (F-P) in optics. Using the same assumptions and extending the ALAT approach of Mei, they developed the mathematical model for linear incident waves propagating over two separated patches of ripples on an otherwise flat bottom. The flat bottom region between two patches is called 'resonator'. The F-P resonance condition is composed of two parts: as Bragg resonance, the incident wavelength must be twice that of the bottom ripples; in addition, the resonator must have a particular length with respect to bottom wavelength. In this condition, the wave energy could be trapped within the resonator, resulting in large amplification of the incident waves and forming standing waves with large amplitude.

The present work aims at studying some of the assumptions of the ALAT, in particular focusing on the wave-bottom interaction. Through numerical simulations we examine in which manner higher-order bottom effects associated with the expression of the bottom boundary condition (BBC) adopted in the mathematical models of Mei [6] and Couston *et al.* [1] may affect the occurrence of the F-P resonance on a particular configuration. The effect of the relative ripple amplitude is also addressed through these numerical simulations, and comparisons with ALAT predictions are analyzed.

II – Mathematical modeling of Fabry-Pérot resonance

The wave problem is expressed in a 2D vertical Cartesian coordinate system (x, z), with x-axis located at the mean free surface level, and z-axis positive upward. We assume sandbars to be parallel to the y-axis and waves propagate along the x direction only (*i.e.* with normal incidence with respect to the sand ripples). Assuming (i) the fluid is incompressible and homogeneous, (ii) the flow is irrotational, and (iii) surface waves are of infinitesimal amplitude, the linear water wave problem (labeled as system A in the following) can be formulated in terms of velocity potential $\phi(x, z, t)$:

$$\phi_{xx} + \phi_{zz} = 0, \quad -\tilde{h}(x) \leq z \leq 0, \tag{1a}$$

$$\phi_{tt} + g\phi_z = 0, \quad z = 0, \tag{1b}$$

$$\tilde{h}_x\phi_x + \phi_z = 0, \quad z = -\tilde{h}(x), \tag{1c}$$

in which subscripts denote partial derivatives, and g is the gravitational acceleration. The free surface elevation $\eta(x, t)$ is related to the velocity potential through the linearized free surface boundary condition (FSBC) $\eta = -\phi_t|_{z=0}/g$. The water depth is considered to be of the form $\tilde{h}(x) = h - \zeta(x)$, where h is the (constant) mean water depth and $\zeta(x)$ is the shape of ripples superimposed on the flat bottom:

$$\zeta = \begin{cases} d\sin\left[k_b(x - x_1^s) - \theta_1\right], & x \in [x_1^s, x_1^e], \\ d\sin\left[k_b(x - x_2^s) - \theta_2\right], & x \in [x_2^s, x_2^e], \\ 0, & \text{elsewhere.} \end{cases} \tag{2}$$

where x_j^s and x_j^e represent the start and the end of patch j ($j = 1, 2$), $L_j = x_j^e - x_j^s = N_j L_b$ ($N_j \in \mathbb{N}$) is used to denote the length of the patch j. k_b is the wave number of the bottom corrugations, the corresponding wavelength is $L_b = 2\pi/L_b$. The resonator length is denoted by $L_r = x_2^s - x_1^e$. θ_j is the initial phase of the j-th patch (chosen to be 0 or π in order to have a continuous bottom shape). Considering the form of Eq. (2), the assumption of bottom ripples of small amplitude (*i.e.* $k_b d \ll 1$ and $d/h \ll 1$) allows to write Eq. (1c) as an approximate BBC, by retaining only the first order terms of its Taylor expansion:

$$-\left(\zeta\phi_x\right)_x + \phi_z = 0, \quad z = -h. \tag{3}$$

Note that Eq. (3) is now applied at the constant elevation $z = -h$. The system composed of Eqs. (1a, 1b, 3) is called system B in the following.

We know from ALAT that the Bragg resonance happens when the incident wave number is $k_B = k_b/2$ (to be clear, the subscript 'B' stands for 'Bragg' and 'b' for 'bottom'). Now the monochromatic incident water waves come from $x = -\infty$ with a wave number $k = k_B + \kappa$, $\kappa \ll k_b$. This means that the incident wave number lies in the vicinity of the Bragg wave number k_B. For the incident wave number k, the corresponding wave angular frequency is obtained by the dispersion relation $\omega = \sqrt{gk\tanh(kh)}$, Bragg resonance condition in frequency is $\omega_B = \sqrt{gk_B\tanh(k_B h)}$, the detuning frequency corresponding to κ is $\Omega = C_g\kappa$, where C_g is the group celerity at the Bragg wave number:

$$C_g = \frac{1}{2}\left(1 + \frac{2k_B h}{\sinh 2k_B h}\right)\frac{\omega_B}{k_B}. \tag{4}$$

Due to the wave-bottom interaction, the amplitude is slow varying. The general solution of F-P resonance over the j-th patch of the linearized system reads

$$\phi = f(z)[\mathcal{A}_j(x', t')e^{-ikx} + \mathcal{B}_j(x', t')e^{ikx}]e^{i\omega t} + c.c., \tag{5}$$

where *c.c.* denotes the complex conjugate, $i = \sqrt{-1}$, x' and t' are the slow variables. $\mathcal{A}_j$, $\mathcal{B}_j$ denote the slowly varying complex amplitudes of the incident and reflected waves over the patch j, the time variation for both of them is simple harmonic motion. Then the time variation can be written explicitly $\mathcal{A}_j = A_j(x')e^{i\Omega t'}$, $\mathcal{B}_j = B_j(x')e^{i\Omega t'}$. $f(z)$ is the vertical structure of the velocity potential:

$$f(z) = -\frac{ig}{2\omega}\frac{\cosh k(h+z)}{\cosh kh}. \tag{6}$$

By using the multiple-scale method, and keeping the leading order terms of the solution, the following system can be obtained:

$$i\Omega\mathcal{A}_j + C_g\frac{\partial\mathcal{A}}{\partial x'} = -\Omega_c e^{i\theta_j}\mathcal{B}_j, \tag{7a}$$

$$i\Omega\mathcal{B}_j - C_g\frac{\partial\mathcal{B}}{\partial x'} = \Omega_c e^{-i\theta_j}\mathcal{A}_j, \tag{7b}$$

where

$$\Omega_c = \frac{\omega_B k_B d}{2\sinh 2k_B h}. \tag{7c}$$

It can be seen that for the flat bottom parts ($\zeta(x) = 0$), $\Omega_c = 0$: the incident and reflected waves propagate at the speed of group velocity without coupling. If only one patch j is considered, the model returns to Mei's theory for Bragg resonance [6]. The (complex) Bragg reflection and transmission coefficients are then obtained analytically as functions of normalized detuning frequency Ω/Ω_c:

$$\mathcal{R}_j^B(\mathcal{P})|_{x_j^s} = \frac{\mathcal{B}(x_j^s, t')}{\mathcal{A}(x_j^s, t')} = \frac{e^{-i\theta_j}\sinh S_j\mathcal{Q}}{\mathcal{Q}\cosh S_j\mathcal{Q} + i\mathcal{P}\sinh S_j\mathcal{Q}}, \tag{8a}$$

$$\mathcal{T}_j^B(\mathcal{P})|_{x_j^e} = \frac{\mathcal{A}(x_j^e, t')}{\mathcal{A}(x_j^s, t')} = \frac{\mathcal{Q}}{\mathcal{Q}\cosh S_j\mathcal{Q} + i\mathcal{P}\sinh S_j\mathcal{Q}} \tag{8b}$$

where

$$\mathcal{P} = \Omega/\Omega_c, \quad \mathcal{Q} = \sqrt{1-\mathcal{P}^2}, \quad S_j = \frac{\Omega_c L_j}{C_g}. \tag{8c}$$

If the following, R_j^B and T_j^B denote the modulus of these coefficients, and α_j^B denotes the complex argument of $\mathcal{R}_j^B$.

If two patches are considered, and the system is solvable thanks to the continuity of the free surface elevation over the resonator area, *i.e.* the amplitude of the incident waves of the second patch equals that of the transmitted wave of the first patch. Thus, the reflection and transmission coefficients for F-P resonance read (see more details in [1]):

$$R^{FP}|_{x_1^s} = \left[\frac{(R_1^B)^2 + (R_2^B)^2 - 2R_1^B R_2^B\cos\gamma}{1 + (R_1^B R_2^B)^2 - 2R_1^B R_2^B\cos\gamma}\right]^{1/2}, \tag{9a}$$

$$T^{FP}|_{x_2^e} = \left\{\frac{\left[1-(R_1^B)^2\right]\left[1-(R_2^B)^2\right]}{1 + (R_1^B R_2^B)^2 - 2R_1^B R_2^B\cos\gamma}\right\}^{1/2}, \tag{9b}$$

where

$$\gamma = \pi - 2\theta_1 + 2k_B L_r - \alpha_1^B - \alpha_2^B. \tag{10}$$

In addition to Bragg resonance condition, the wave energy will be trapped within the resonator when $\gamma = 2m\pi$ ($m \in \mathbb{N}$). This is denoted as F-P resonance condition in which the standing waves with highest achievable amplitude are expected between two patches. The non-dimensional amplitude of the standing waves within the resonator is defined as enhancement factor E^{FP} and can be computed as follows [1]:

$$E^{FP} = \frac{|\mathcal{A}(x_1^e, t')| + |\mathcal{B}(x_1^e, t')|}{|\mathcal{A}(x_1^s, t')|} = \left(1 + R_2^B\right) \frac{T^{FP}}{T_2^B}. \tag{11}$$

The water depth affects the results through entering S in Eqs. (8). C_g is related to the mean water depth h. Ω_c is not only affected by the water depth but also by the amplitude of the ripples d. The relation between the relative ripple amplitude d/h and the enhancement factor E^{FP} is plotted in Fig. 1.

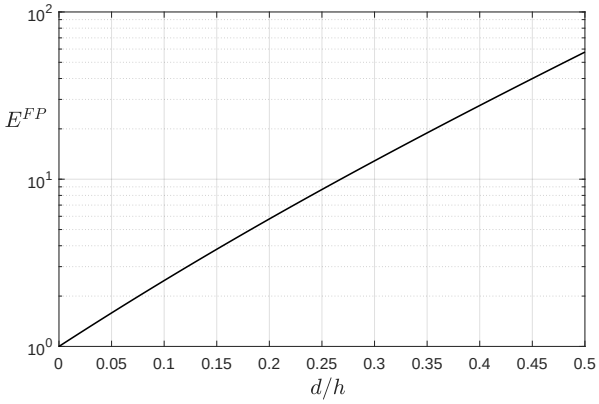

Figure 1: Enhancement factor E^{FP} as a function of the relative amplitude of the bottom ripples d/h, other parameters such as N_1, N_2, k_bL_r, k_bh and k_bd are chosen to be identical to the ones used in the figure 6 of [1].

In this asymptotic linear analytical theory (ALAT), the enhancement factor E^{FP} increases exponentially with the relative ripple amplitude d/h, as shown in Fig. 1, achieving values of about 4 around $d/h = 0.15$ and exceeding 10 for $d/h = 0.3$. Such local amplification of incident waves might be of interest for coastal engineering applications in certain cases, for example harnessing wave energy.

However, it remains to be tested whether such large amplification can be really achieved in practice, especially the effects associated with the assumptions used in ALAT, *i.e.* the assumptions on the smallness of surface waves and on the smallness of the bottom ripples, needs to be studied. In the current study, we focus on the assumption on the bottom ripples amplitude by using an efficient potential linear wave model (presented in the next section). The test conditions to be simulated are identical to the ones used in the figure 6 of [1], except for the relative amplitude of bottom ripples d/h which varies in our study from 0.1 to 0.2.

III – The numerical model: whispers3D

The numerical simulations are performed with a highly accurate code, called whispers-3D, currently developed at Ecole Centrale Marseille and Irphé lab. It solves the fully nonlinear potential wave problem with variable bottom conditions, in the form of two

coupled nonlinear equations, corresponding to the two nonlinear free surface boundary conditions (FSBC). In dimensional form for the case of a single horizontal dimension [10], they are expressed as:

$$\eta_t = -\eta_x \tilde{\phi}_x + \tilde{w}\left[1 + (\eta_x)^2\right], \tag{12a}$$

$$\tilde{\phi}_t = -g\eta - \frac{1}{2}(\tilde{\phi}_x)^2 + \frac{1}{2}\tilde{w}^2\left[1 + (\eta_x)^2\right], \tag{12b}$$

where $\tilde{\phi}(x,t) \equiv \phi(x, z = \eta(x,t), t)$ is the free surface velocity potential and $\tilde{w}(x,t) \equiv \phi_z(x, z = \eta(x,t), t)$ is the vertical velocity at the free surface.

In order to march Eqs. (12) in time, the vertical velocity $\tilde{w}(x,t)$ has to be determined as a function of $(\eta(x,t), \tilde{\phi}(x,t))$, which corresponds to a so-called 'Dirichlet-to-Neumann (DtN)' problem. The modeling approach used is presented in previous works [9, 7] and summarized hereafter. Following Tian and Sato [8], a spectral approach is used in the vertical to approximate the velocity potential. Using the set of orthogonal Chebyshev polynomials of the first kind, denoted $T_n(s), n = 0, 1, ..., N_T$, with $s \in [-1, 1]$, as an expansion basis, the potential is approximated at any given time t (omitted for brevity hereafter) as

$$\phi(x,z) = \varphi(x,s) \approx \sum_{n=0}^{N_T} a_n(x) T_n(s), \tag{13}$$

where $s(x,z,t)$ is the scaled vertical coordinate allowing to map the water column $z \in [-\tilde{h}(x), \eta(x,t)]$ into the fixed range $s \in [-1, 1]$, and the a_n coefficients $(n = 0, 1, ..., N_T)$ depend upon the local abscissa x (and time t).

The main steps involved in solving the DtN problem and marching Eqs. (12) in time are summarized as follows: (i) first, the system of governing equations composed of the Laplace equation, a Dirichlet FSBC on the potential and the BBC is expressed in the (x, s) coordinate system, (ii) then, the approximation given in Eq. (13) is inserted into those equations, (iii) the so-called Chebyshev-tau method, a variant of the Galerkin method, is used to project the Laplace equation onto the T_n polynomials for $n = 0, 1, ..., N_T - 2$ eliminating the s coordinate and giving a set on $N_T - 1$ equations on the a_n coefficients at each location x, (iv) two additional equations are obtained by considering the Dirichlet FSBC and the BBC so that a system of $N_T + 1$ linear equations with $N_T + 1$ unknowns $(a_n, n = 0, ..., N_T)$ at each abscissa is formed, (v) once this linear system is solved for the a_n coefficients, the free surface vertical velocity at t is obtained as

$$\tilde{w}(x,t) = \frac{2}{\tilde{h}(x) + \eta(x,t)} \sum_{n=1}^{N_T} a_n(x,t) n^2, \tag{14}$$

allowing Eqs. (12) to be integrated in time.

In the current study, the linearized version of whispers3D is used. The linearization is achieved by (i) ignoring the nonlinear terms in Eqs. (12), (ii) solving the DtN problem on a domain bounded by the level $z = 0$ (instead of $z = \eta(x,t)$), and (iii) replacing the total water depth $\tilde{h}(x) + \eta(x,t)$ in Eq. (14) by the still water depth $\tilde{h}(x)$. Then, two different variants are considered: one with the exact BBC (system A), and one with the approximate BBC (system B). In all cases horizontal derivatives are approximated using fourth-order finite difference formulas using stencils of 5 nodes on a regular grid, and an explicit third-order Runge-Kutta scheme (SSP-RK3) is used for time marching.

IV – Numerical simulations of Fabry-Pérot resonance

IV – 1 General settings of the numerical simulations

In the present work, we simulate the F-P resonance case as was chosen in the figure 6 of [1] with two the systems A and B. The original set-up is recalled here: $N_1 = 11$ ripples, $N_2 = 15$ ripples, $\theta_1 = \theta_2 = 0$, $k_b h = 1.64$, $d/h = 0.1$, $a/h = 10^{-5}$ and resonator length $L_r/L_b = 5.5$ (corresponding to $m = 5$ in Eq. (10)). To investigate the effect associated with the assumption of small ripple amplitude, we further studied the case $d/h = 0.2$. In practice, we choose $L_b = 0.5$ m for the wavelength of the ripples (giving a theoretical Bragg wavelength $L_B = 2L_b = 1$ m).

In terms of the numerical parameters, two relaxation zones with $3L_B$ in length are set to generate regular waves on one side and absorb them on the other side. The numerical basin is uniformly meshed with $\Delta x = L_b/64$ ($= L_B/128$), the time step is $\Delta t = T_B/256$ resulting in a Courant-Friedriechs-Lewy number $CFL = 0.5$. These discretization parameters were selected after a convergence study. Meanwhile, the time required to reach an established periodic regime depends on the relative ripple amplitude.

In the following, the theoretical results $\mathcal{A}$ and $\mathcal{B}$, corresponding to the solution of ALAT shown in Eqs. (7), are the complex wave amplitudes, the modulus of the solutions $|A|$ and $|B|$ correspond to the envelopes of the amplitudes, excluding time variations as well as fast spatial variations. On the flat bottom zones, standing waves are expected resulting in the amplitude envelopes to be constant. In addition, because of the reflection from the ripples downwave, the value of normalized amplitude envelope falls in the range $[1, 2]$ before the first patch. Meanwhile, due to the conservation of energy, the amplitude envelope of transmitted waves is less than 1 after the second patch. Between the two patches, the wave energy is trapped in the resonator area, thus a high constant level is expected from the ALAT results over this zone.

IV – 2 Perfectly tuned cases with different ripple amplitudes

We start with the same case as in the figure 6 of [1] with $d/h = 0.1$, in order to validate our numerical model. Based on ALAT, for the incident wave number $k = k_B$, we find: global reflection coefficient $R^{FP} \approx 0.245$, enhancement factor $E^{FP} \approx 2.476$ (resonator), and transmission coefficient is $T^{FP} \approx 0.970$. Note that $(R^{FP})^2 + (T^{FP})^2 = 1$. Considering two patches separately, the results of ALAT for Bragg resonance in Eqs. (8) give: reflection coefficient of the first patch ($N_1 = 11$) $R_1^B \approx 0.597$ and reflection coefficient of the second patch ($N_2 = 15$) $R_2^B \approx 0.734$. Both are larger than the reflection coefficient in F-P resonance, due to the fact that the energy is trapped within the resonator.

The comparison between the theoretical result and simulated results (with systems A and B) is shown in Fig. 2a. The fast spatial variation of the envelope is kept in the simulated results, corresponding to the envelope of the free surface elevation (or to the local amplitude of the free surface oscillation).

It is seen that in the case $d/h = 0.1$ the agreement between the simulated results and the theoretical result is reasonably good. It is also observed that the two numerical systems give almost the same results. Only in very local scale can some differences be seen. This justifies that the approximation on the BBC in the current case is acceptable. The reflection of the patches is stronger in the simulations than predicted by ALAT. The simulated reflection coefficient is $R^{FP} \approx 0.329$ with System A, whereas the enhancement factor $E^{FP} \approx 2.385$ and the transmission coefficient $T^{FP} \approx 0.944$ are slightly smaller than ALAT predictions.

For the case $d/h = 0.2$, we doubled the ripple amplitude while holding the water depth unchanged. As is shown in Fig. 1, the enhancement factor increases exponentially as the relative ripple amplitude increases. The wave-bottom interaction is more significant in this case. When the resonance takes place, according to ALAT, the reflection coefficient $R^{FP} \approx 0.462$, the enhancement factor $E^{FP} \approx 5.785$ and the transmission coefficient $T^{FP} \approx 0.887$. However, Fig. 2b shows that the resonance does not take place in this case. In addition, system A with exact BBC and system B with approximate BBC show different results. The system B with the approximate BBC (which is also adopted in ALAT) give even smaller enhancement factor within the resonator. Neither system A nor system B is close to the ALAT prediction (bold line). Incident waves are almost fully reflected by the ripples resulting in $R^{FP} \approx 1$. The enhancement factor is $E^{FP} \approx 1.711$ with system A.

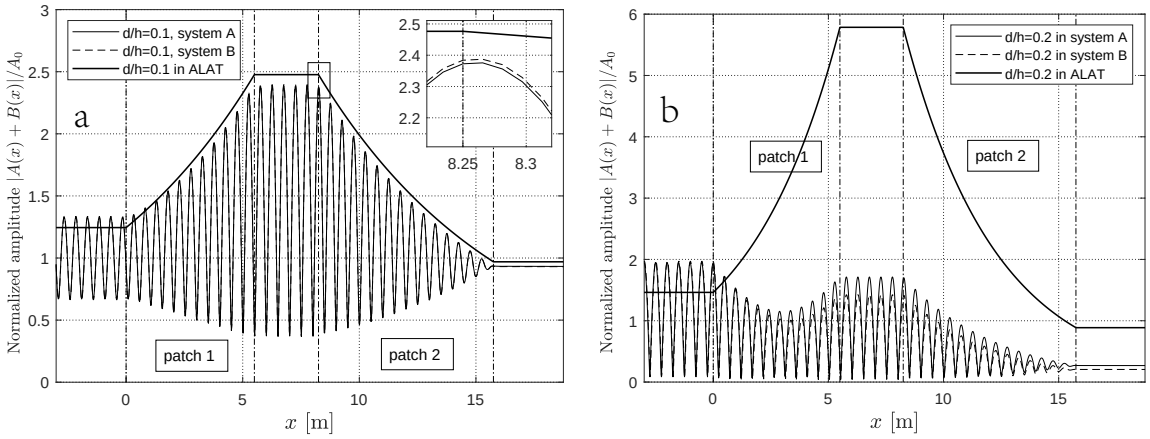

Figure 2: Computed envelope of the free surface elevation at the end of the simulations of system A and B, $t = 200T$ for the case $d/h = 0.1$ (left panel), $t = 900T$ for the case $d/h = 0.2$ (right panel). The results of ALAT which are the envelopes of the amplitude are also superimposed.

IV – 3 Slightly detuned incident waves for the case $d/h = 0.2$

Do our results indicate that, when the amplitude of the bottom ripples is relatively large, the F-P resonance completely disappears and that incident waves will be strongly reflected by the bottom ripples? This question is interesting because of the significant difference between the expected value from ALAT $E^{FP} \approx 5.785$ and the simulated result $E^{FP} \approx 1.711$ (system A) in the case $d/h = 0.2$, and the difference is greater when d/h is larger.

In seeking an explanation of this behavior, the so-called 'wave number downshift' drew our attention. As was observed in the early experiments [3], in the case with large ripple amplitude $d/h = 0.16$, the strongest Bragg reflection of incident waves did not take place when the theoretical Bragg resonance condition was met, *i.e.* the incident wave number $k = k_B$, but it happened when the incident waves were of slightly smaller wave number. This phenomenon was also observed in the numerical study of [5] who simulated the experiments of Davies & Heathershaw [3] using a highly accurate model. In [5] a high-order spectral (HOS) method was adopted to solve the nonlinear water wave problem up to an arbitrary order M (in their study, $M = 4$ was used). In their work

the simulated results showed limited but clear downshift of wave number when compared to ALAT predictions, while in terms of reflection coefficients R^B, their simulated results were in good agreement with ALAT predictions.

This motivated us to perform a series of runs by slightly perturbating the incident wave number around the theoretical value k_B. The results shown in Fig. 3 illustrate that, with relatively large bottom ripples, the incident waves are strongly amplified within the resonator and the reflection coefficient reaches its minimum value when the incident wave number is slightly smaller than k_B. The downshift of the wave number is limited, as was observed in the simulations of Bragg resonance [5], whereas it largely affects the result in the present F-P resonance. This can be explained by the fact that the F-P resonance condition is more 'strict' than Bragg resonance condition: the F-P resonance only manifests for a relatively narrow range of wave numbers. When the incident wave number falls outside this range, the wave energy will be largely reflected by the ripples. The slight deviation from the F-P resonance condition due to 'wave number downshift' is thus of significant importance.

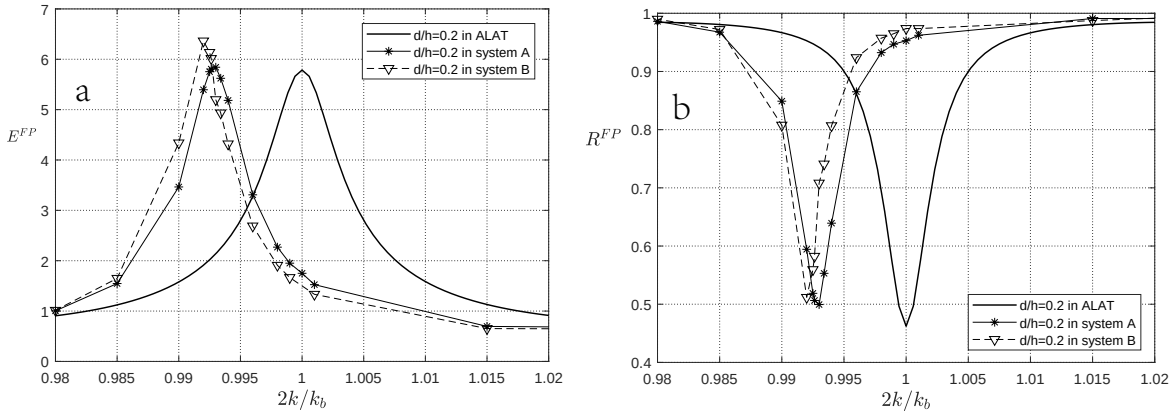

Figure 3: The enhancement factor (left panel) and the reflection coefficient (right panel) as functions of incident wave number k, normalized by $k_B = k_b/2$ for the case $d/h = 0.2$. The duration of the simulations is $t = 900T$.

In system A with exact BBC, the maximum enhancement factor $E^{FP} \approx 5.805$ is observed at $2k/k_b \approx 0.99263$, and the corresponding reflection coefficient is $R^{FP} \approx 0.5065$. These values are in better agreement with the ALAT prediction than those of system B. Regarding system B with approximate BBC, the minimum reflection happens for $2k/k_b \approx 0.992$, the enhancement is overestimated $E^{FP} \approx 6.363$ and the reflection coefficient $R^{FP} \approx 0.512$ is smaller than expected in ALAT. The degree of wave number downshift is different only by 1% for k/k_B, but the differences it makes is obvious. Both systems A and B show a similar wave number downshift but with small differences in the magnitude of downshift. This is due to the difference in the formulation of the BBC (the unique difference between the two systems) and implies, as the resonance curves are rather sharp, that for a same incident wave number the amplification of wave from system A and B can be significant different (in particular in the vicinity of the resonance condition).

As a further illustration of the occurrence of F-P resonance with slightly detuned incident wave number, the comparison between the envelope of wave amplitude from ALAT and the envelopes of the free surface elevation from systems A and B is given in Fig. 4 for the case $d/h = 0.2$. The simulations are done with an incident wave number

tuned to the resonating wave number for system A, namely $k/k_B = 0.99263$. Again, the differences between system A and system B mainly result from the different degree of frequency downshift between the two systems (as this wave number is close to, but different from, the resonating wave number of system B).

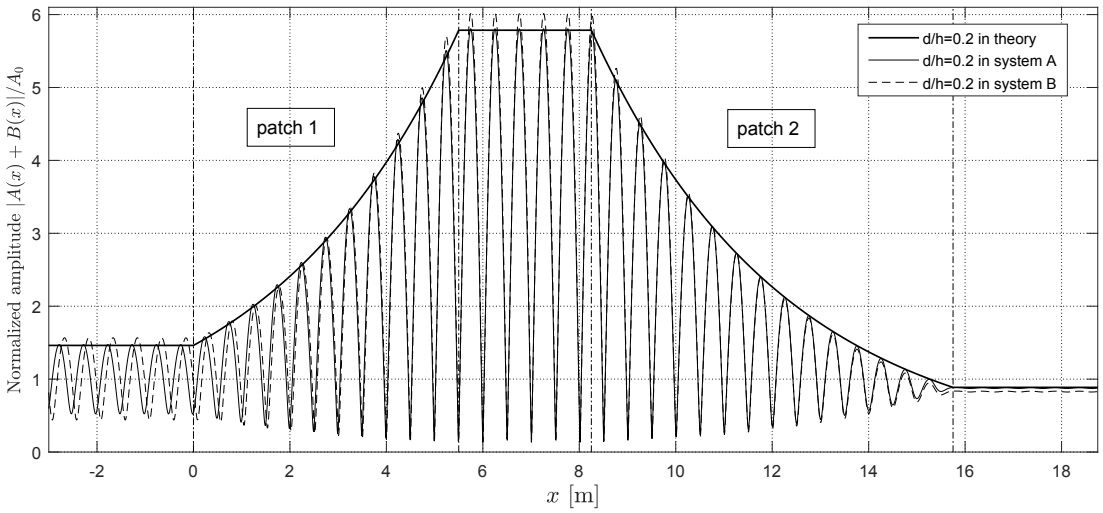

Figure 4: Computed envelope of the free surface elevation at the end of the simulations of systems A and B, $t = 900T$ for the case $d/h = 0.2$ and $k/k_B = 0.99263$. The result of ALAT which is the envelope of the amplitude is also superimposed.

V – Conclusions

Recently, Couston *et al.* (2015) [1] studied the resonance of water waves using two distinct sets of bottom corrugations, in analogy with Fabry-Pérot resonance in optics by using an asymptotic linear analytical theory (ALAT). The ALAT solution is derived based on the assumptions that incident monochromatic water waves are of small amplitudes and that the bottom ripple amplitudes are small too. In the present study, we examined the higher-order effects of BBC by using the linearized version of a highly accurate code (whispers3D) solving the fully nonlinear potential and dispersive wave problem. The motivation is that, in the coastal areas as the water depth decreases, the nonlinear effect of wave-bottom interaction becomes more and more important. According to ALAT prediction, the enhancement factor should increase exponentially as the relative ripple amplitude d/h increases, which may result in very large amplification of incident waves between the two patches when the resonance conditions are met.

Two cases following the work of Couston *et al.* (2015) [1] were analyzed and simulated, with different relative ripple amplitudes $d/h = 0.1$ and 0.2. The first case with $d/h = 0.1$ is identical to the one used in [1], it validates our numerical model to the corrugated bottom condition. Two systems with exact BBC and approximate BBC are tested. They show very similar results in the case $d/h = 0.1$, the resonance is indeed realized, even though in simulations $E^{FP} \approx 2.385$ is smaller than expected under the F-P condition. However, in the case $d/h = 0.2$ the resonance does not manifest when the incident wave number $k = k_B$, and two systems show differences. This can be explained by the so-called 'wave number downshift' in Bragg resonance, meaning that the resonance takes place for an incident wave number slightly lower than k_B. For the F-P resonance this effect makes a

significant difference because the resonance condition is 'strict', especially when the d/h is large enough. A number of simulations have been conducted in order to demonstrate this wave number downshift and to find the shifted F-P resonance condition. The differences between the system A (with exact BBC) and system B (with approximate BBC) become considerable, and result (at least partially) from the different degree of wave number downshift between the two systems.

With the shifted incident wave number, the F-P resonance can be realized in the numerical model with a satisfying agreement with ALAT results regarding the enhancement factor of wave amplitude. In system A, the enhancement factor $E^{FP} \approx 5.805$ agrees well with the predicted value from ALAT $E^{FP} \approx 5.785$. In system B, although the enhancement factor is overestimated, the wave number downshift is also well described. This means that the wave number downshift effect is already present when the BBC is approximated at first order. Last but not least, given the good agreement in the case with large ripple amplitude obtained by taking the downshift into consideration, the analysis and understanding of the first case with $d/h = 0.1$ can be improved in the same way.

Future work will address the study the higher relative ripples' amplitude, as well as the effects introduced by taking into consideration waves of finite amplitude (free surface nonlinearity), and how these effects affect the occurrence of F-P resonance.

References

[1] L. A. Couston, Q. C. Guo, M. Chamanzar, and M. R. Alam. Fabry-Perot resonance of water waves. *Phys. Rev. E*, 92(4):043015, 2015.

[2] A. G. Davies. On the interaction between surface-waves and undulations on the seabed. *J. Mar. Res.*, 40(2):331–368, 1982.

[3] A. G. Davies and A. D. Heathershaw. Surface-wave propagation over sinusoidally varying topography. *J. Fluid Mech.*, 144:419–443, 1984.

[4] A. D. Heathershaw. Seabed-wave resonance and sand bar growth. *Nature*, 296(5855):343–345, 1982.

[5] Y. M. Liu and D. K. P. Yue. On generalized Bragg scattering of surface waves by bottom ripples. *J. Fluid Mech.*, 356:297–326, 1998.

[6] C. C. Mei. Resonant reflection of surface water waves by periodic sandbars. *J. Fluid Mech.*, 152:315–335, 1985.

[7] C. Raoult, M. Benoit, and M. L. Yates. Validation of a fully nonlinear and dispersive wave model with laboratory non-breaking experiments. *Coastal Eng.*, 114:194–207, 2016.

[8] Y. Tian and S. Sato. A numerical model on the interaction between nearshore nonlinear waves and strong currents. *Coast. Eng. J.*, 50(4):369–395, 2008.

[9] M. L. Yates and M. Benoit. Accuracy and efficiency of two numerical methods of solving the potential flow problem for highly nonlinear and dispersive water waves. *Int. J. Numer. Methods Fluids*, 77(10):616–640, 2015.

[10] V. E. Zakharov. Stability of periodic waves of finite amplitude on the surface of a deep fluid. *J. Appl. Mech. Tech. Phys.*, 9(2):190–194, 1968.